ANL-LTR-CERT-11-001

Summary of Multiphase Measurements from Contactor ERT Facility FY11 Experiments

Chemical Sciences and Engineering Division

About Argonne National Laboratory

Argonne is a U.S. Department of Energy laboratory managed by UChicago Argonne, LLC under contract DE-AC02-06CH11357. The Laboratory's main facility is outside Chicago, at 9700 South Cass Avenue, Argonne, Illinois 60439. For information about Argonne and its pioneering science and technology programs, see www.anl.gov.

Availability of This Report

This report is available, at no cost, at http://www.osti.gov/bridge. It is also available on paper to the U.S. Department of Energy and its contractors, for a processing fee, from:

U.S. Department of Energy
Office of Scientific and Technical Information
P.O. Box 62
Oak Ridge, TN 37831-0062
phone (865) 576-8401
fax (865) 576-5728
reports@adonis.osti.gov

ANL-LTR-CERT-11-001

Summary of Multiphase Measurements from Contactor ERT Facility FY11 Experiments

prepared by
Kent E. Wardle
Chemical Sciences and Engineering Division, Argonne National Laboratory

September 30, 2011

work sponsored by
U.S. Department of Energy,
Office of Nuclear Energy, Science and Technology

Summary of Multiphase Measurements from Contactor ERT Facility FY11 Experiments (FCR&D Project FTAN11SW0511)

Kent E. Wardle*
Chemical Sciences and Engineering Division
Argonne National Laboratory
Argonne, IL 60439, U.S.A.

30 September 2011

1 Introduction

Development of computational science based methods for separations process R&D requires the application of advanced experimental techniques to provide the type of data necessary for validation of detailed physical models. For complex multiphase flows in solvent extraction equipment, optical techniques have limited applicability due to the opacity of the flow and advanced interrogation techniques are needed. A facility has been established to apply electrical resistance tomography (ERT), a non-intrusive phase fraction measurement technique, to an engineering-scale annular centrifugal contactor. In addition, high-speed imaging is also being employed to provide additional insight as well as aid in the development and validation of the technique. This report summarizes the results of single phase and liquid–liquid measurements from FY11 experiments in the Contactor ERT (CERT) facility.

2 Experimental Setup

A brief description of the facility and equipment will be given here. Please refer to the previous report for milestone M41SW051102 for additional description of the facility along with the original test plan.

*kwardle@anl.gov

2.1 ERT Instrumented Contactor

An annular centrifugal contactor obtained from CINC Industries having a 5-inch diameter, hanging rotor (model CINC-V5) has been customized with an acrylic housing and rotor to allow for optical access as well as provide electrical insulating vessel walls for ERT measurements. The sensor arrays include 8 planes of 18 electrodes (16 active plus 2 ground) in vertical arrays and one 32 electrode circumferential array position near the top of the vanes (bottom of the rotor). These electrodes are connected to a p2+ ERT System from Industrial Tomography Systems to acquire both point voltage measurements and tomographic reconstructions for measurement of liquid phase fractions under multiphase operation with a single liquid phase (and air) or two liquid phases. A picture of the instrumented contactor is shown in Figure 1. The contactor unit is also equipped with a changeable bottom plate with attached vanes of various configurations including: CINC's standard 8 curved vanes and straight vane plates with 4,6, and 8 vanes. Throughout this report, these vane configurations will be denoted as CV, 4V, 6V, and 8V. The plates used for the tests reported here were an opaque fluoropolymer material but transparent, acrylic vane plates have

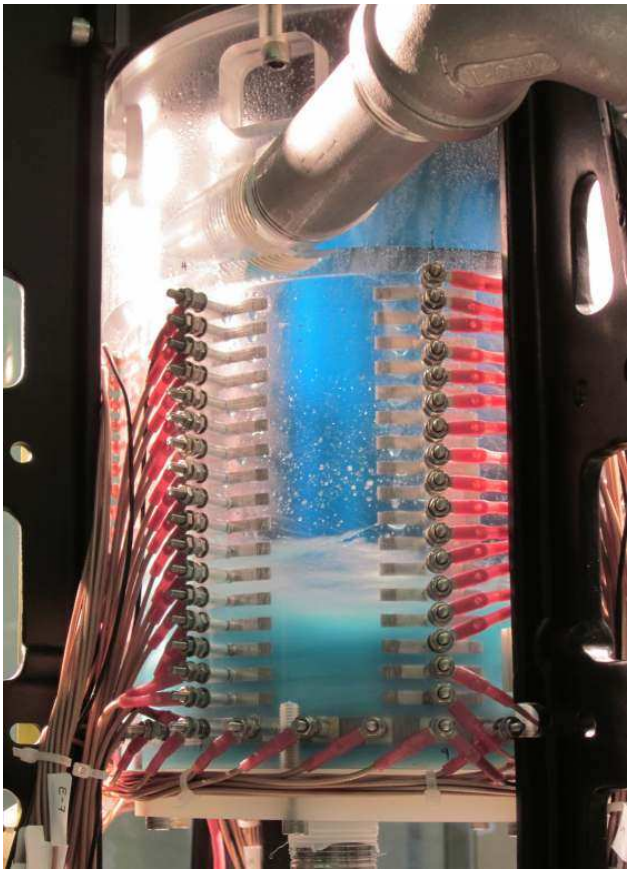

Figure 1: Snapshot of electrode instrumented CINC V5 contactor during liquid-liquid operation. The aqueous phase is dyed blue. The liquid inside the rotor can be seen in the interior of the contactor above the lighter blue mixed phases in the foreground.

been purchased for future tests and visual validation of ERT results.

Unless otherwise stated, the results presented here are for operation of the contactor at 1800 RPM. The rotor speed was confirmed and recorded by laser tachometer. Rotor power as reported by the contactor's main control unit and accessed via the LabView data acquisition system was also recorded along with other system data such as feed/effluent tank masses and feed flow meters.

2.2 Process Solutions

The process solutions for the liquid–liquid tests were changed slightly from the original test plan which was to use ferric nitrate in the aqueous phase as the 'salting out' agent to boost the extraction of nitrate and the corresponding electrical conductivity of the organic phase. It was discovered that iron(III) extracts and precipitates out mono- and dibutyl phosphate degradation products. While new solvent is used for the test, it was chosen to use aluminum nitrate instead to avoid precipitate issues in the future as a relatively large volume of solvent is needed for this contactor and is intended for reuse. In addition, while aluminum itself does not extract, it is a better salting agent than iron nitrate. The composition of liquid–liquid phase pair used for these tests consisted of:

Aqueous Phase: 37.5 wt% aluminum nitrate (1M) in 8 wt% nitric acid (1M)

Organic Phase: 40 vol% tributyl phosphate (lab grade) in dodecane (technical grade mixture of isomers)

As the aluminum nitrate solution is colorless, a very small amount of methylene blue was also added to the aqueous phase. It was found that this coloring agent stayed in the aqueous phase. Test tube samples of the dyed aqueous phase in constant contact with the organic phase did exhibit diminishing color over several months. Methylene blue is known to degrade on exposure to light so this is not entirely unexpected and will not have any impact on the experiments.

Following preparation of the two 'clean' solutions, initial pre-equilibration of the phases was done by continuous processing through the contactor unit for a period of about 1 hour. The masses of the feed tanks were monitored and the extraction of solutes (primarily nitrate ions) from the aqueous phase to the organic phase and the corresponding change in densities could be observed. The two phases were each pumped at approximately 3 L/min (O/A$\approx$1). Given the initial volume of 50 L for each, the 60 minute run represented about 4 volume turnovers of the feed tank. Plots of the feed tanks for the two phases are shown in Figure 2. The initial linear decrease in both cases is the period after the pumps have been turned on but return flow from the contactor has not yet occurred—this provides a check of the initial flow rates.

The measured densities and electrical conductivities of the two liquid phases following equilibration are given in Table 1. The measured organic phase conductivity was somewhat lower than expected from earlier batch tests, but was considered sufficient for ERT measurements. Note that the conductivities are several orders of magnitude different. The challenges with making multi-phase conductivity measurements for such disparate values are described later on in this report.

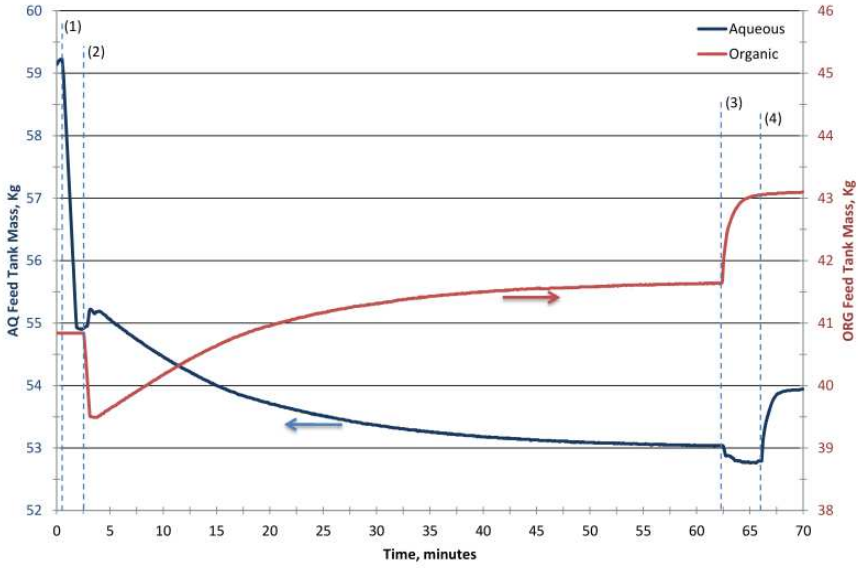

Figure 2: Plots of feed tank mass during pre-equilibration of liquid–liquid phases. Extraction of nitrates (and some water) from the aqueous phase result in the observed mass change. Labeled times are (1) aqueous pump start, (2) organic pump start, (3) organic pump stop, and (4) aqueous pump stop.

Table 1: Density and electrical conductivity for liquid–liquid phases.

Property	Aqueous Phase	Organic Phase
Density, gm/cm^3	1.172	0.855
Electrical conductivity	169 mS/cm	7.6 μS/cm

2.3 ERT System

A snapshot of the electrical tomography system's control unit is shown in Figure 3. This unit is capable of measurements on eight channels of 16 working electrodes (128 electrodes). In addition, as described in the previous report, it can be operated in two main modes: (1) tomographic mode* and (2) electrode scan mode. The main settings controlling the quality of data acquisition in terms of reducing signal to noise and measurement uncertainty are the injection current (ranging from 0.1–75 mA) and injection frequency (typical value is 9600 Hz). For single-phase, tap water operation values of 25 mA and 9600 Hz were typically used. For liquid–liquid measurements, and injection current of 50 mA or even 75 mA was used. Various values of injection frequency were tested, but this seemed to have little effect on electrode scans as were the focus of the two liquid tests to date.

2.4 High-speed Camera

High speed imaging of the mixing zone as seen through the side of the transparent contactor housing was also performed to verify liquid height measurements from the tomography system and provide additional insight into single- and two-fluid operation. The camera was a Redlake (IDT) MotionPro X5plus model capable of 500 frame/second imaging at a resolution of 2352x1728 (4 megapixels) and increased speed at reduced resolution. Typical measurements such as those shown later in Figure 6 consisted of 1000 frames at 500 frames/second (duration of 2.0 s of flow) which were then averaged to give the resulting images. Longer videos at much reduced framerate were also taken to observe the dynamics of long transients (∼20 s).

*The tomographic measurements can be taken in real (resistance tomography) or real/complex mode (impedance tomography). While only resistance tomography has been performed thus far and is reported here, future work using impedance tomography could yield additional data for organic continuous conditions.

Figure 3: Control unit for p2+ electrical resistance tomography (ERT) system from Industrial Tomography Systems.

3 Summary of Results

3.1 Single-phase Tests

It has been observed in previous studies that the apparent volume of fluid in the annular mixing zone for given conditions differs for different mixing vane geometries [1, 2]. Taking advantage of our real time data acquisition system, an experimental procedure was devised by which the relative volume differences for the different configurations could be quantitatively measured. This was done by starting the contactor and feed lines empty and with a known mass in the feed tank (50.0 kg). After starting the rotor and data acquisition system, the pump was started at a flow rate of 5 L/min and the system allowed to reach steady-state. The flow rate was then successively increased to 10 L/min and 15 L/min. Because continuous recycling was used (contactor outflow returned to feed tank), the feed tank mass was constant at steady-state and the difference relative to the starting mass was then equal to the 'system' mass. In this case, the 'system' being defined as the feedline, the contactor mixing zone, rotor, collector rings and exit lines. While it is not possible to get more than an estimate for the mixing zone volume from this data, if the same test is repeated for a different mixing vane configuration, the difference in the steady-state tank mass is equal to just the difference in the mixing zone mass for the two vane types. This follows from the reasonable assumption that the liquid volumes outside of the contactor (i.e. the feedlines and exit lines) are equivalent for the same flow conditions as well as the assumption that the rotor liquid volume is itself not dependent on the mixing vane geometry. While this last assumption is consistent with previous knowledge of contactor hydrodynamics, its validity needs to be verified. Using the 4V case as the baseline for comparison, tests were done at the three different flow rates (5, 10, 15 L/min) for the three additional vane types: 6V, 8V, and CV. Table 2 gives the results of these tests. The dependence on vane type is consistent with previous observations with increasing number of vanes having decreasing liquid volume and curved vanes having less volume than straight ones of equivalent number. It can also be seen that as vane number increases, the dependence on flow rate decreases leading to diminishing volume increases for larger inlet flow

Table 2: Steady-state 'system' volume measurements for the four different mixing vane configurations at three different flow rates (5, 10, 15 L/min) with those for the 6V, 8V, and CV shown relative to the 4V case. The last line of the table shows the rate of flow loss (in ml/min) out of the light phase outlet (LO) at the highest flow rate, 15 L/min.

Flow Rate, L/min ↓	System Volume, L	System Vol. Relative to 4V, L		
Vane Type →	**4V**	**6V**	**8V**	**CV**
5	3.66	-0.06	-0.06	-0.11
10	4.09	-0.11	-0.13	-0.25
15	4.42	-0.15	-0.21	-0.34
ml/min loss to LO @ 15 L/min	62.23	25.17	11.36	7.28

rates.

As pointed out above, the assignment of these relative differences in system volume to mixing zone volume changes alone is based on the previously accepted assumption that the volume of liquid in the rotor depends only on the rotor geometry, rotation rate, and total inlet flow rate and NOT on the mixing zone configuration. However, to the author's knowledge no previous zero-point flow rate tests for different mixing vane types have been reported to confirm this assumption. The present tests results shown in the bottom line of Table 2 show that the amount of flow which was measured exiting from the light phase exit (that is, flow that went over the light phase weir) was slightly different for the four different vane cases and followed the same trends as the liquid volume (more LO flow for more mixing zone volume). Tests were done with stepwise increases of the single-phase feed flow rate and observation of the point at which flow began to exit the light-phase outlet port—the so-called zero-point. This was done for each of the vane types. An example zero-point experimental run for the 6V case is shown in Figure 4. The labels and highlighted regions denote the stepwise increase of the feed flow rate. For this case, measurable flow from the light phase (organic) outlet is first seen at a feed flow rate of 13.5 L/min. Plots of the total inlet flow versus the amount of flow from the light phase exit for each of the vane configurations is shown in Figure 5. It is very clear that there is a dependency of the zero-point flow rate on mixing vane geometry with the trends following those seen for the mixing zone volume (Table 2) and also the annular liquid height as shown later. While the explanation for this is as yet somewhat unclear, this demonstrates that the flow inside the rotor is not wholly independent of the mixing zone.

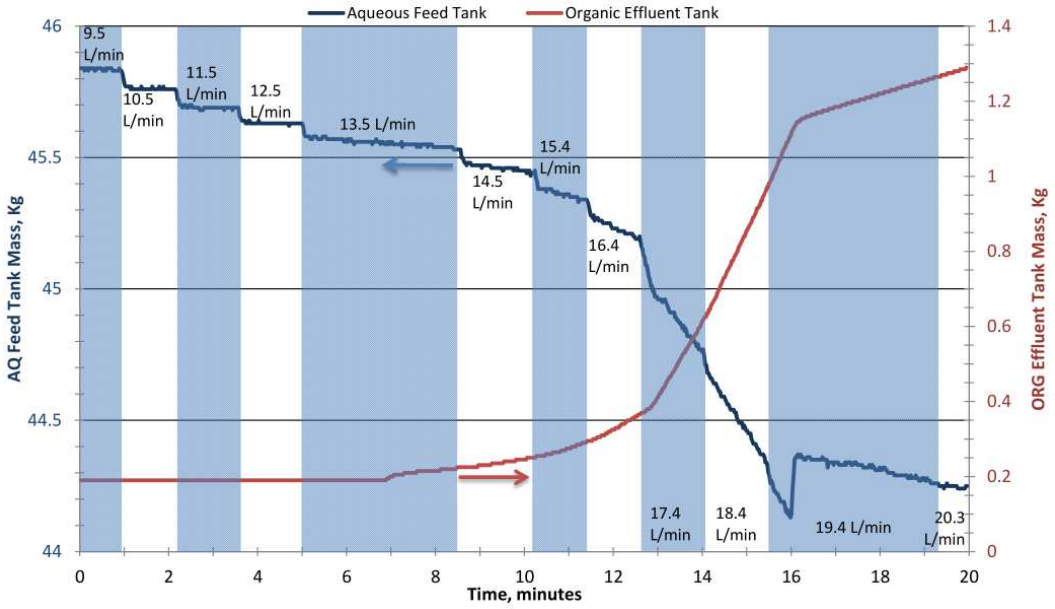

Figure 4: Example zero-point flow rate test for the 6V geometry. Text labels and highlighted regions show the incremental total feed flow rate (calculated from pump setting and calibration). The discontinuity just after t=16 min is an apparent result of siphon formation in the aqueous underflow.

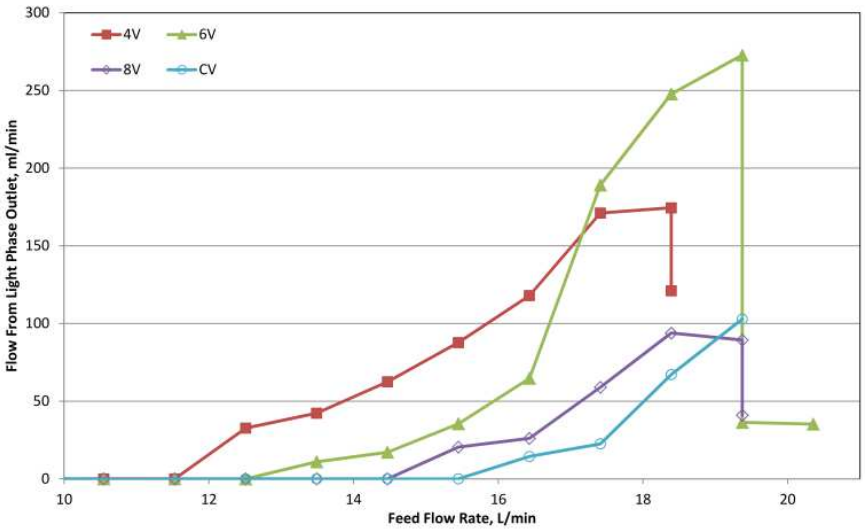

Figure 5: Plots of total flow versus flow from light phase outlet for the four vane types tested showing the relative zero-points for each case.

Also apparent in Figure 4, near t=16 minutes there is a sudden jump in the aqueous feed tank mass (resulting from a sudden decrease in holdup in the contactor) which is also marked by a sudden decrease in the rate of flow from the light phase outlet. This was not a result of any input changes (e.g. decrease in feed rate or increase in rotor speed) and occurred almost half a minute following the increase of inlet flow to 19.4 L/min. This can also be seen in the resulting data Figure 5. While not as substantial as the 6V case, a similar discontinuity was seen for the 8V case at the same flow rate and one also for the 4V case at a lower flow rate (18.4 L/min). Interestingly, the CV case did not experience this type of discontinuity over the range of flow rates tested. Based on previous experimental observations and computational simulations [3, 4] it is thought that this sudden shift is the result of a siphon formation in the aqueous underflow region and above the aqueous weir. CINC Industries contactors have cap that holds the changeable upper weir in place and forms a narrow flow area above the weir and four outlet channels for flow to exit. As the flow rate increases to a point where the small space above the aqueous weir under the weir cap fills with water and seals off the outlet channels, the pressure above the weir suddenly drops resulting in a shift of the liquid surface inside the rotor and the observed discharge of aqueous phase volume and subsequent decrease in outflow from the light phase side. Note that it was not possible to take data for the 4V above 18.4 L/min as the annular mixing zone had filled up past the inlets. In addition, backflow out the empty organic phase inlet line (which slopes downward from the contactor and empties into the organic effluent tank in this setup) was observed for the 4V case at this flowrate. The amount of backflow was visually noted to be greater than that coming from the light phase outlet from the contactor and thus the lower data point for the 4V case at this flow rate (18.4 L/min) is somewhat questionable–the actual rate should be considerably lower. For the other vane types, the organic phase inlet line was filled with water and the corresponding valve closed such that back flow out of the mixing zone and down the organic inlet line was not possible. It is not clear why the 6V case shows a shift to higher light phase outlet flow at 17.4 L/min as compared to the other

cases—it appears that for some reason this particular run experienced a higher pressure drop in the aqueous underflow region resulting in the increased flow over the light phase weir.

3.1.1 High-speed Imaging

In addition to the flow monitoring and system volume comparisons at the three different flow rates as described above, high-speed digital imaging was also conducted for each of these cases. Time-averaged images for each of the vane types at 10 L/min are shown in Figure 6. The upper row shows images from a non-instrumented housing and the lower row the same measurements repeated for the ERT-instrumented housing. The consistency between the two confirms that the insertion of the electrodes had no noticeable effect on the flow.[†] Similar to previous observations for the V2 contactor, there is a clear decrease in annular liquid height for increasing vane number with 4V $>$ 6V $>$ 8V $>$ CV. Despite the uncertainty regarding vane effects on rotor liquid volume, this observation also follows the same trend as seen in the Table 2 measurements.

3.1.2 Electrode Measurements of Annular Liquid Height

The same trends are seen from the conductivity measurements from the vertical electrode arrays (Figure 7) in the annular region coupled with a more quantitative comparison of the relative volume fraction (in this case, the amount of entrained air) that this technique provides. For reference, the inlets are well above the topmost electrode. Some circumferential asymmetry is apparent. The flow is entering via a single inlet and for many conditions (particularly for low annular volumes as in 8V and CV) the resulting liquid level is asymmetric—low downstream of the inlet flow penetration and high on the opposite side. In particular, looking at the CV case (Figure 7(d)) for the different planes (rows descending) in plane 1 there is a maximum in liquid height due to the incoming liquid stream on the housing wall. Around plane 3 or 4 there is a minimum which climbs back to a higher state at planes 7 and 8. For reference, the view shown in the lower row of Figure 6 is on the side opposite the inlet and shows planes 5 and 6 on the right and left, respectively. The diminished dependency of the liquid height on flow rate for the 8V and CV cases as mentioned in respect to Table 2 is also observable.

From all this we confirm that mixing vane geometry has a significant effect on annular liquid height and mixing zone volume. How these differences translate to liquid–liquid mixing and stage efficiency is a question that we anticipate ongoing two-phase measurements will be able to assess. It may be that increased mixing is beneficial to extraction efficiency in creating greater interfacial area for extraction. On the other hand, there may be cases where mixing is too vigorous and small droplets are formed which do not separate in the rotor and consequently exit with the opposing phase—so-called ‘other phase carryover‘—contributing to a decrease in stage efficiency.

[†]Electrodes were inset into the housing wall and edge gaps epoxied and sanded/polished such that the inner housing wall was as smooth and undisturbed as possible.

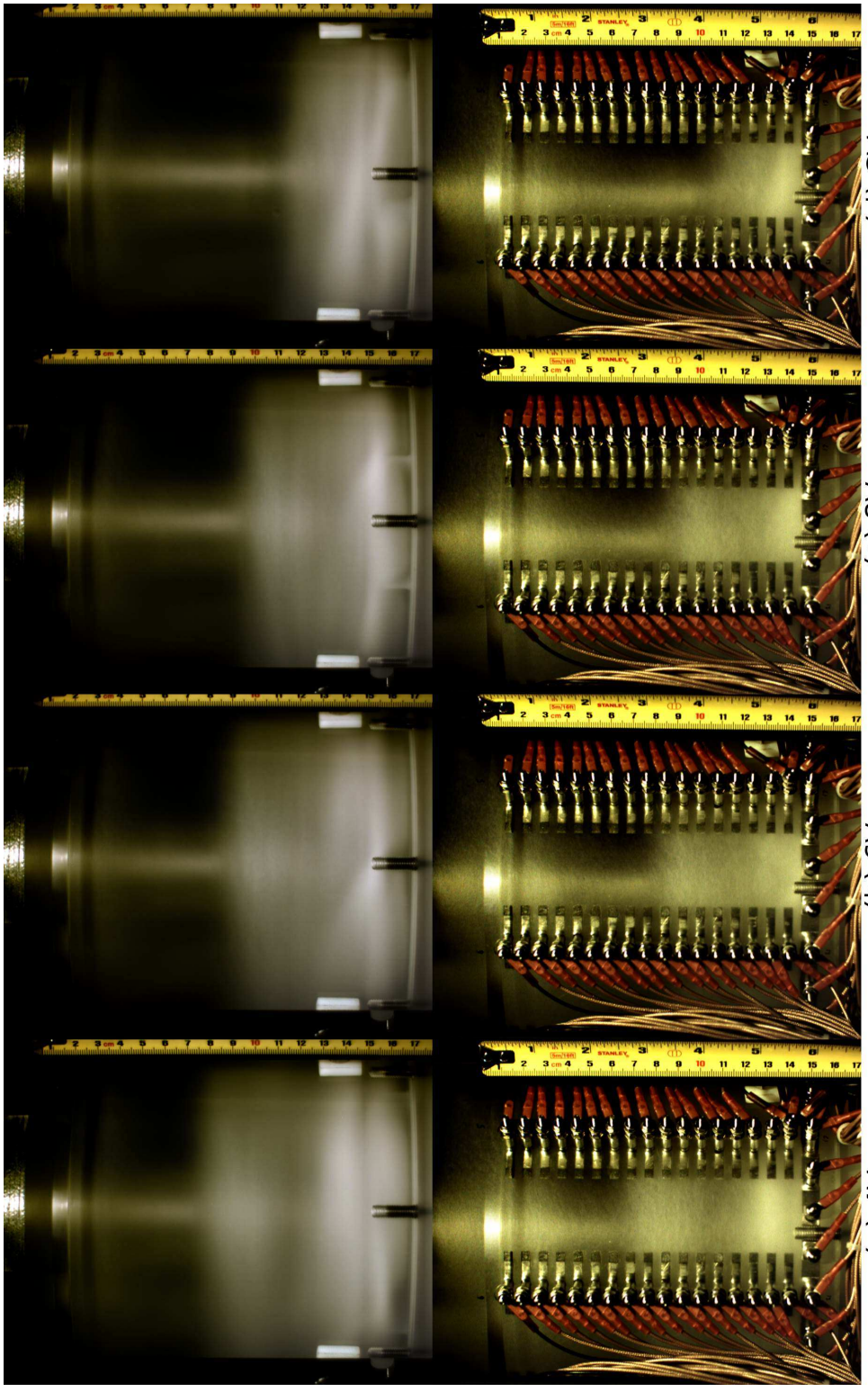

Figure 6: Time-averaged images of steady-state flow at 10 L/min for each of the four vane types tested. Lower row shows same measurements with ERT-instrumented housing. Note that the position of the tape measure is not the same for the two rows but consistent across vane types.

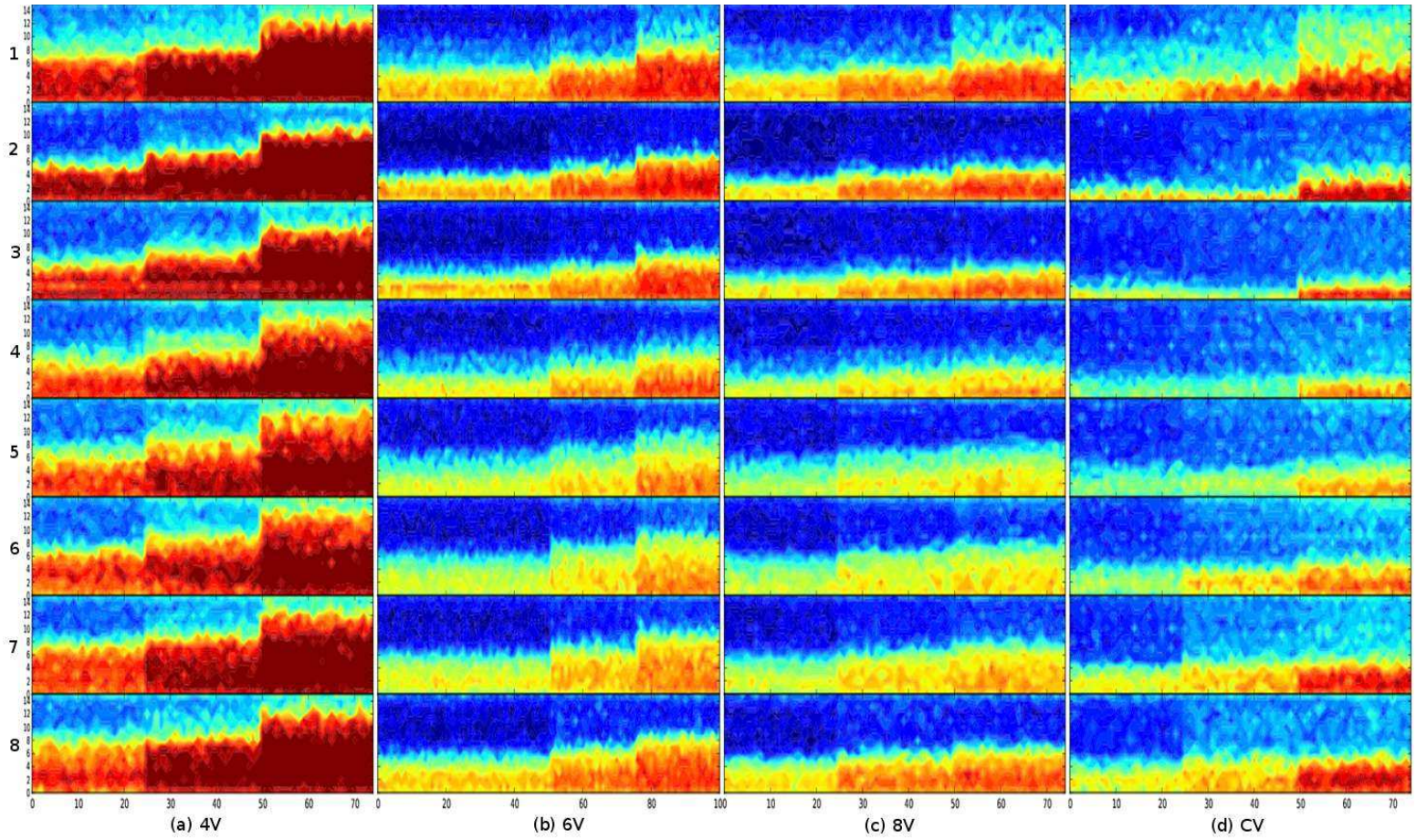

Figure 7: Plots of water volume fraction as measured by 8 vertical planes of electrodes (rows, plane number on left) with plane 1 being the first downstream (wrt spinning rotor) of the heavy phase inlet, followed by plane 2 and so on around the circumference of the housing with plane 8 being just upstream of the inlet penetration. Measurements for each vane case are for the three flow rates (5, 10, and 15 L/min) for roughly equal durations. Horizontal numbering shows time as data frames (∼4–6 s per frame).

3.1.3 Circular Plane ERT: Comparison of Reconstruction Techniques

While the annular electrode measurements as presented above are useful for quantification of the volume fraction along the housing wall in the annulus, they give only a series of point measurements. True tomography, takes a complex series of multipoint measurements and uses this to reconstruct (using a finite element method)[‡] a 2D map of volume fraction in the measurement plane. While the narrow annular gap makes useful tomographic results difficult for the linear arrays, the single circumferential array of 32 electrodes locate around the lower portion of the housing at the top of the mixing vanes (bottom of the rotor) is specifically suited for this. To date only measurements of the 4V geometry have been performed.

Tomographic measurements for the 4V geometry at 10 L/min (and 1800 RPM) were taken for tap water operation using the p2+ ERT system. The data rate was approximately 1 Hz meaning that each data set was an average over a period of about 1 s. While the data acquisition software has a reconstruction scheme capable of real-time image reconstruction, it has poor spatial resolution. Data were exported and post-processed using two different ERT tools: (1) a software package also provided by ITS that uses an algorithm called sensitivity conjugate gradient (SCG) [5] to reconstruct the tomographic image and (2) an open-source ERT package based in MATLAB called EIDORS [6] that uses similar techniques. While the SCG software restricts users to a limited number of meshes, the EIDORS packages allows user construction of the mesh using other meshing tools (an open-source tetrahedral mesh generator called Netgen was used) that can enable explicit specification of vessel internals—in this case, the housing vanes. Figure 8 shows a comparison of one data frame from the 4V case reconstructed with SCG and EIDORS on comparable meshes as well as one with EIDORS using a mesh with explicit vanes (Figure 8(c)). Disregarding the scaling and color map differences between the SCG and EIDORS cases, the computed phase fraction profile

[‡]The reconstruction entails solution on a mesh of the inverse problem—that is, given a set of boundary measurements, what is the cross-sectional volume fraction field (as indicated by electrical conductivity) that would give rise to those boundary values.

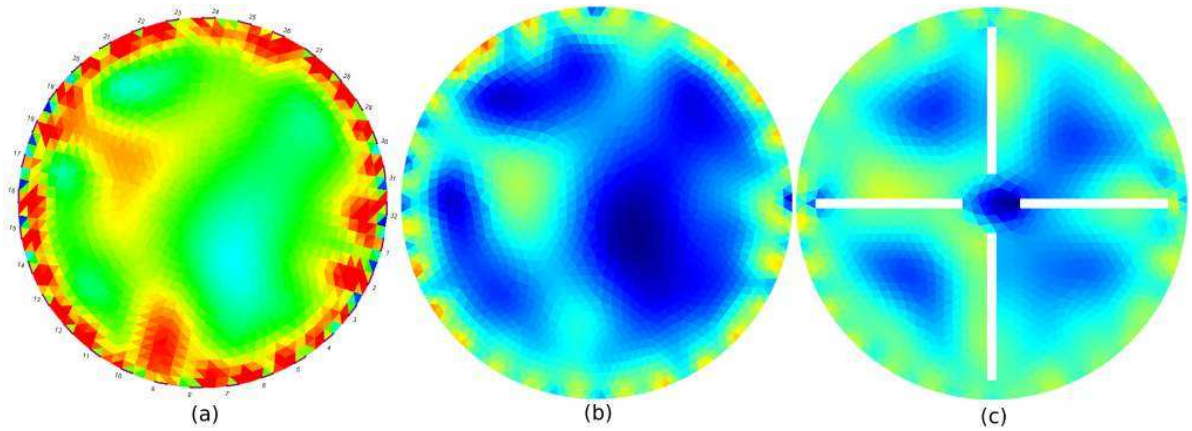

Figure 8: Comparison of ERT reconstructions from measurements (4V) on the 32 electrode circular array near the top of the vanes (bottom of the rotor) . Reconstructions were done using (a) SCG software, (b) EIDORS package, and (c) EIDORS package with explicitly meshed vanes.

is essentially the same. Explicit meshing of the vanes results in a significantly different reconstruction, and one that matches more closely with the expected field based on previous high-speed imaging of the 4V configuration in the smaller CINC V2 contactor [2]. While visual confirmation of this volume fraction distribution was not possible at the time of this writing, acrylic vane plates for the V5 contactor in the CERT facility are now available and early work for FY12 will focus on validation of these ERT measurements and reconstructions. Also, for this data to be used in CFD model validation, it will be critical to understand the effect of the reconstruction mesh and algorithms on the resulting 'data.'

3.2 Liquid-liquid Tests

The majority of work during this FY has focused on exploring single phase behavior for the different vane configurations and preparing for liquid–liquid tests. Thus far, using only the 4V configuration, a number of liquid-liquid tests have been conducted. Unfortunately, the range of flow rates that could be tested was limited by excessive foaming that occurred on the organic outlet. It was found that above ∼4–5 L/min organic flow, foam was generated at some point *downstream of the contactor* and steadily crept back up the organic outlet and pushed up out of the vent tube just outside the contactor. As it was possible to see down into the vent tube as well as through the translucent liquid lines, it was possible to confirm that the foam was not being generated in the contactor or collector rings but rather was due to the configuration of the outlet line. While some care was taken in design of the outlet lines to avoid unnecessary inner diameter changes in the tubing such as through the use of bore-through fittings and full-bore three way valves, a sharp 90^o bend near the outlet was required and this is a likely cause. Also, since TBP acts as a surfactant and a 40 vol% mixture is being used it is perhaps more susceptible to foaming than lesser fractions of TBP. Early efforts for FY12 will be made to redesign this section of the setup and widen the parameter space of organic flow rates available for testing.

3.2.1 Steady-state Liquid Height

Comparison was made between mixing zone behavior for liquid–liquid operation and that of single-phase operation. Furthermore, given that the aqueous phase had a higher density than water (∼17% higher—see Table 1) it was also possible to observe the effects of fluid property changes on single-phase operation. Figure 9 shows comparison of mixing zone images for the 4V geometry at a total flow rate of 5 LPM for water, aqueous phase, and liquid–liquid flow with O/A = 0.33, 1, and 3. The bottom row shows time-averages and the top instantaneous snapshots (at a point of minimum liquid height). As compared to tap water, the liquid height for the aqueous phase only operation at the same flow rate was slightly higher (∼1 cm). As the O/A ratio increased (from 0 for aqueous only), the minimum liquid height slightly decreased though the average was comparable due to increasing fluctuations. The O/A of 3 was substantially higher than the other cases both in terms of the typical minimum liquid height (Figure 9(e), top) but also there were very significant, periodic liquid height excursions. The rate of these oscillations (based on approximate minimums from the high-speed images) was 3.7 Hz with a magnitude of oscillation greater than 7 cm.

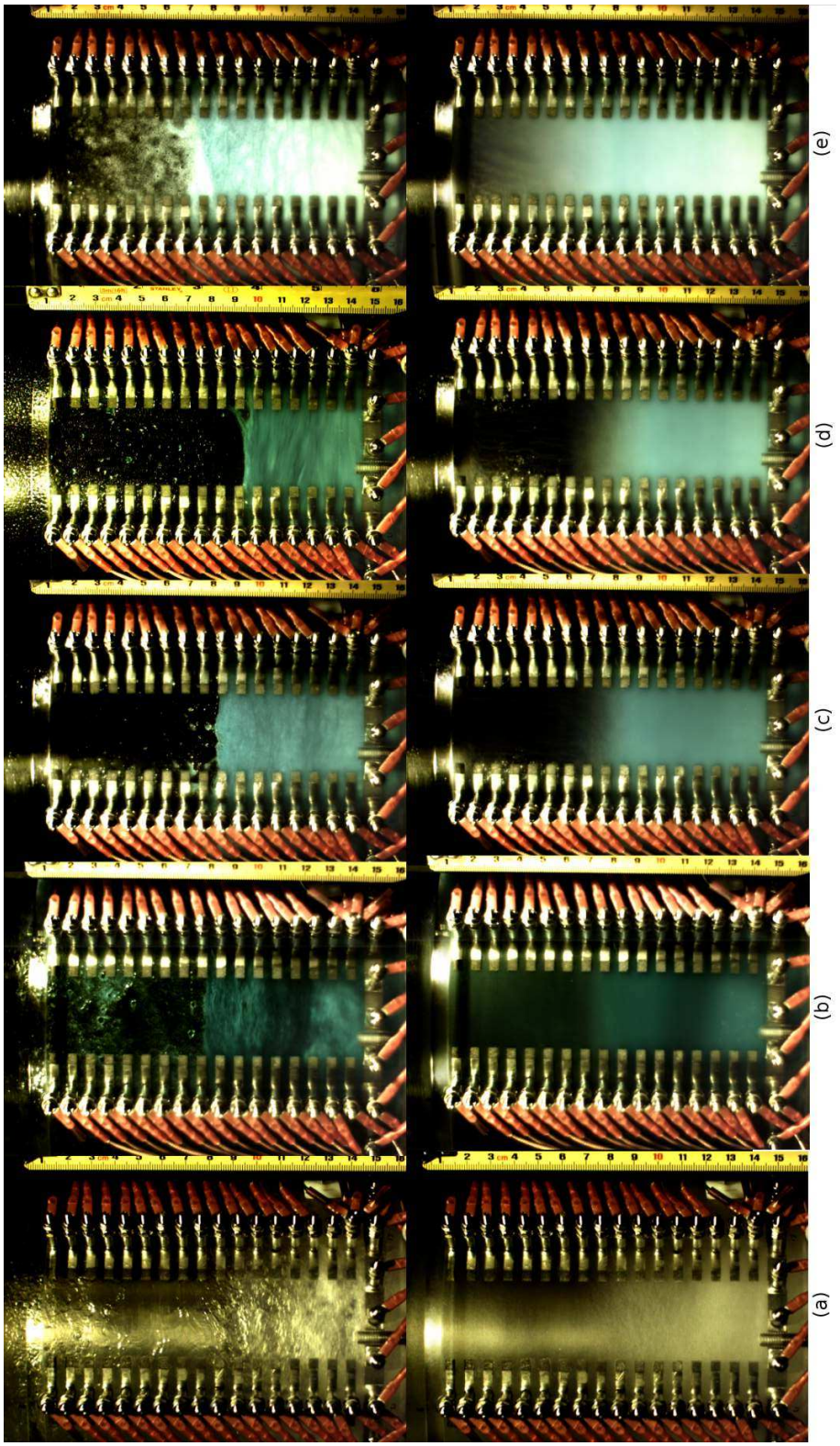

Figure 9: Comparison of 4V configuration at 5 LPM total flow for (a) tap water, (b) O/A = 0 (aqueous phase only), (c) O/A = 0.33, (d) O/A = 1, and (e) O/A = 3 for phases shown in Table 1. Top row shows an instantaneous snapshot at a point of minimum liquid height and bottom row shows a time-averaged image.

3.2.2 Transient Behavior and ERT Measurements

Along with the steady-state behavior, the transitional behavior for flow going from aqueous continuous to organic continuous and vice-versa was also explored. Several experimental runs including electrode scan measurements for the vertical arrays were done in which the test was started from a stationary, all-aqueous liquid height and after reaching steady aqueous flow, the organic flow was cycled on and off twice. Plots of the tank volumes for each phase of such a liquid–liquid run at O/A of 1 and total feed flow rate of 5 L/min are shown in Figure 10. The corresponding liquid volume fraction measurement from electrode scans over a single electrode array (# 6—this is the array on the left in the images in Figure 9) for the same test period are shown in Figure 11. From Figure 10, it is interesting to note that when the organic flow begins, aqueous in the system is displaced (returning to the feed tank) and when the organic flow is shut off following steady-state liquid–liquid operation such as at t=5 s, the aqueous volume in the system does not fully rebound—the difference being the volume of organic remaining in the rotor. It may be possible to use this value for the residual organic to quantify weir performance or as an additional comparison between vane types.

The electrode measured volume fraction data (Figure 11) shows that soon after the organic phase reached the contactor (frame 59, 137), there was a brief transition period (∼10 s) and then sharp inversion to organic continuous flow and the measurement appeared to 'drop out' (e.g. the period beginning at ∼frame 65 and later at frame ∼142). When the organic phase is turned off (∼frame 100, 175) there is a brief transition period and the signal returns. Note that the data rate for the single plane measurements was approximately 1 frame every 2 seconds. In terms of the flow behavior, the transition to organic continuous was very smooth with only a gradual shift in the

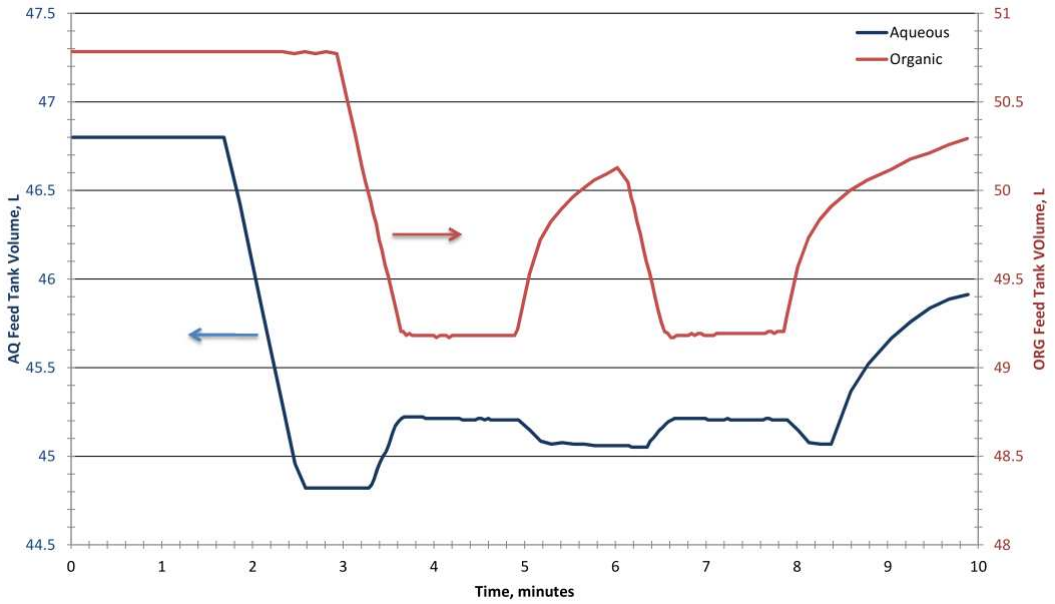

Figure 10: Plot of feed tank volumes for liquid–liquid test at O/A = 1 in which the organic feed was cycled on and off twice.

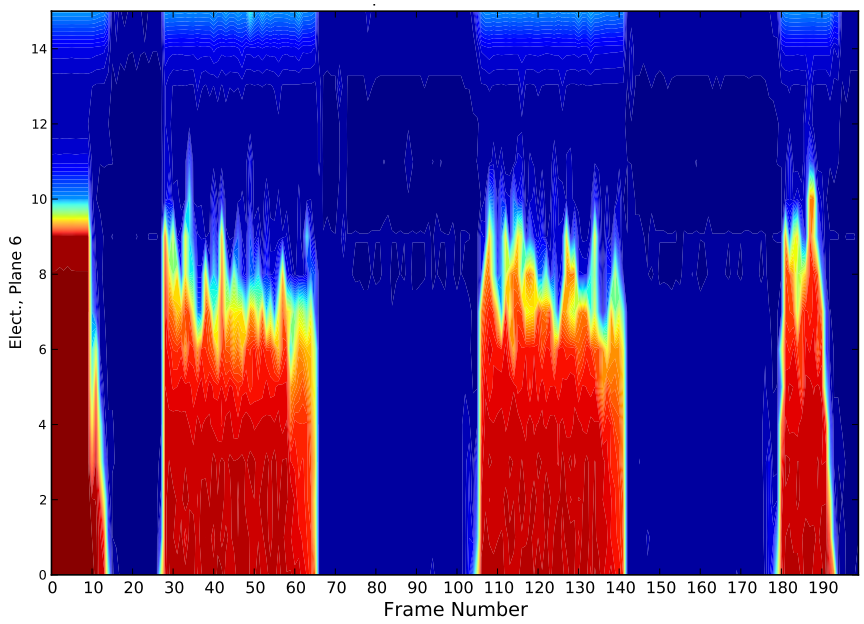

Figure 11: Plot of liquid phase 'fraction' from electrode scan measurements (voltage relative to ground) on array #6 for the test shown in Figure 10.

coloration of the mixture and only a minimal increase in liquid height (though the total flow rate had doubled). The transition from organic continuous operation to aqueous only flow when the organic flow was shut off, on the other hand, was quite different. Video was shot over a duration of 20 s to observe the entire transition. After the organic flow was shut off, the liquid in the mixing zone volume gradually goes through a minimum (occurring $\sim$10 s after organic stoppage—so low it is almost to the bottom of the rotor—then over just a few seconds (3–4 s) the liquid level rises up back to the steady, aqueous only flow value, which as has already been mentioned is comparable to the level at full liquid–liquid flow (though the flow rate is only half the amount).

Unlike the O/A=1 case, for O/A=0.33 the flow remained aqueous continuous allowing continuous data from the electrode measurements as shown in Figure 12. The drop in liquid height beginning at frame 10 is real and corresponds to the emptying of the mixing zone after the rotor is turned on before the aqueous phase pump is started. While the data shows a slight decrease in the conductivity of the dispersion during organic flow periods, it is not particularly marked.

Due to the enormous disparity in conductivity between the two liquid phases, there are challenges to three phase conductivity measurements and discrimination between organic and air, which relative to the aqueous phase, both have essentially the same conductivity—zero. We are working with the tomography system vendor's technical support staff to determine a measurement scheme that will better allow three phase discrimination. For aqueous continuous operation, measurements of the overall liquid height are feasible. Discrimination for quantification of individual volume fractions for the aqueous and organic phases requires a different approach from that taken for computing liquid volume fraction relative to air. In that case, since the conductivity of the other phase (air) is zero it is reasonable to assume the voltage response to varying volume fractions

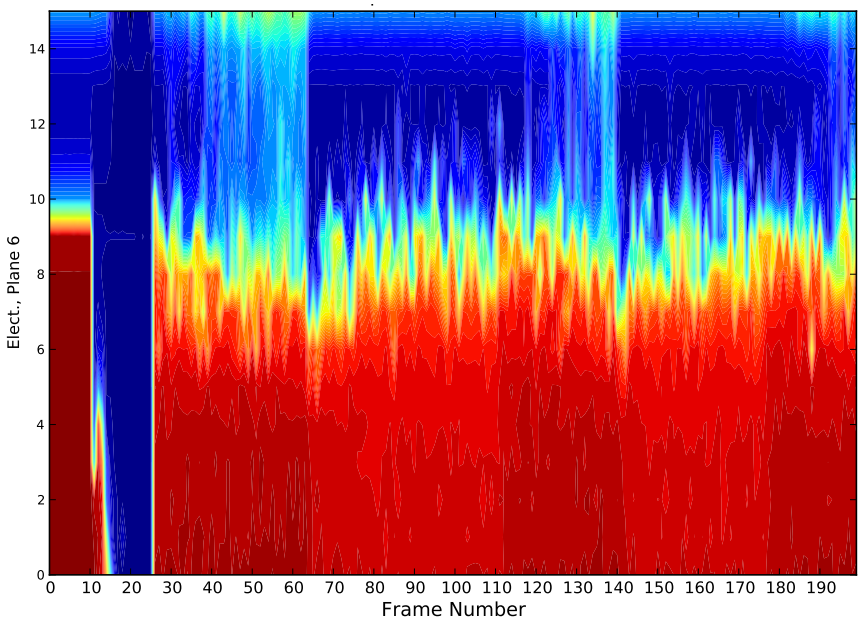

Figure 12: Plot of liquid phase 'fraction' from electrode scan measurements on array #6 for a test similar to the one shown in Figure 10 but for an O/A = 0.33.

is linear. As one might guess, the conductivity of an aqueous–organic dispersion such as this in which the electrical conductivity of the organic phase is small but non-zero does not appear to be a linear function. It may be that the proper functionality given minimal assumptions can be derived from transport theory. Work along these lines will be part of FY12 efforts. In addition, no three-phase ERT measurements of circular plane have been conducted as yet, but similar challenges are expected there.

Despite the challenges in absolute quantification of the multiphase volume fraction from this technique, it is very promising. Furthermore, even given the challenges it is still possible to use the technique for quantitative relative comparisons between different vane configurations. Early FY12 efforts will focus on this, taking advantage of the newly acquired transparent vane plates to provide visual confirmation of results.

References

1. Wardle, K.E., Allen, T.R., Anderson, M.H., Swaney, R.E. (2009) Analysis of the effect of mixing vane geometry on the flow in an annular centrifugal contactor. AICHE J., 55: 2244.

2. Wardle, K.E., Allen, T.R., Anderson, M.H., Swaney, R.E. (2010) Experimental study of the hydraulic operation of an annular centrifugal contactor with various mixing vane configurations. AICHE J., 56: 1960.

3. Gandhir, A., Wardle, K.E. (2011) CFD analysis of fluid flow above the upper weir of an annular centrifugal contactor. Sep. Sci. Technol.: (in press).

4. Wardle, K.E., Allen, T.R., Swaney, R.E. (2009) CFD simulation of the separation zone of an annular centrifugal contactor. Sep. Sci. Technol., 44: 517.

5. Wang, M. (2002) Inverse solutions for electrical impedance tomography based on conjugate gradients methods. Meas. Sci. Technol., 13: 101.

6. Adler, A., Lionheart, W.R.B. (2006) Uses and abuses of EIDORS: an extensible software base for EIT. Physiol. Meas., 27: S25.

Chemical Sciences and Engineering Division
Argonne National Laboratory
9700 South Cass Avenue, Bldg. 205
Argonne, IL 60439

www.anl.gov